

Scalable architecture for Atomtronics flux qubits

S. Safaei,^{1,2} B. Grémaud,^{2,1,3,4} R. Dumke,^{1,5,2} L.-C. Kwek,^{1,6,7,2} L. Amico,^{8,9,1} and C. Miniatura^{2,1,3,5,10,7}

¹*Centre for Quantum Technologies, National University of Singapore, 3 Science Drive 2, 117543 Singapore*

²*MajuLab, CNRS-UNS-NUS-NTU International Joint Research Unit, UMI 3654, Singapore*

³*Physics Department, Faculty of Science, National University of Singapore, 2 Science Drive 3, 117551 Singapore*

⁴*Laboratoire Kastler Brossel, Ecole Normale Supérieure CNRS, UPMC; 4 Place Jussieu 75005 Paris, France*

⁵*Division of Physics and Applied Physics, School of Physical and Mathematical Sciences,*

Nanyang Technological University, 21 Nanyang Link, Singapore 637371

⁶*National Institute of Education and Institute of Advanced Studies,*

Nanyang Technological University, 1 Nanyang Walk, Singapore 637616

⁷*Institute of Advanced Studies, Nanyang Technological University, 60 Nanyang View, Singapore 639673, Singapore*

⁸*INFN-Laboratori Nazionali del Sud, INFN, via S. Sofia 62, 95123 Catania, Italy.*

⁹*CNR-MATIS-IMM & Dipartimento di Fisica e Astronomia, Via S. Sofia 64, 95127 Catania, Italy*

¹⁰*INLN, Université de Nice-Sophia Antipolis, CNRS; 1361 route des Lucioles, 06560 Valbonne, France*

Through a combination of laser beams, we engineer a two-dimensional optical lattice of Mexican hat potentials able to host atoms in its ring-shaped wells. When tunneling can be ignored (at high laser intensities), we show that a well-defined qubit can be associated to atoms trapped in each of the rings. Each of these two-level systems can be manipulated by a suitable configuration of Raman laser beams imprinting a synthetic flux onto each Mexican hat cell of the lattice. Overall, the system forms a scalable architecture for Atomtronics flux qubits.

Atomtronics is an emerging field in quantum technology. It defines a new route for the exploitation of quantum coherence in cold-atoms-matter-wave systems [1–3]. The favourable decoherence/dissipation rates and the high controllability/flexibility make Atomtronics very attractive both to enlarge the scope of quantum simulators and to conceive quantum devices with a new concept. If several elementary circuits have already been realized, both in classical and quantum electronics [4–8], a crucial step forward to exploit the potentialities of Atomtronics is to provide possible solutions for scalable circuits. Here, we present a scheme for a scalable Atomtronics circuit that can be applied in quantum information protocols. Through a specific laser configuration, we create the host for a two-dimensional (2D) array of Atomtronics ring qubits. We demonstrate how each qubit can be addressed within the current quantum optics technology.

As one of the most important themes implying the entire field of quantum technology, qubits can be physically implemented through a variety of solutions exploiting different platforms [9–14]. Solid-state realizations, like the mesoscopic superconductivity-based and semi-conducting quantum dots-based ones, allow the construction of fast gates (nanoseconds) which, however, need to operate in short time scales (microseconds) to fight different sources of decoherence/dissipation. An important advantage of such configurations is that they can benefit from the scalability provided by the highly-developed lithographic techniques. On the other way round, atomic qubits realized by hyperfine states of cold atoms confined in optical lattices have very long storage and coherence times (fraction of second). Single-site addressability is however a main issue challenging the implementation of quantum gates. For such systems, the scalability has been achieved, consistently with the diffraction limit of

the laser light confining potential [15].

Atomtronics flux qubits are seeking to combine the macroscopic quantum coherence of the Josephson junctions flux qubits with the cold atom advantages [16–18]. Similar to the logic applied in quantum electronics, such devices are based on the phenomenology implied by the Atomtronics QUantum Interference Device (AQUID, the atomic counterpart of the SQUID) in which ring-shaped Bose-Einstein condensates (BEC) with broken Galilean invariance are used. The two-level system is based on clockwise and anti-clockwise atomic currents obtained by applying an effective gauge field to the system [19]. In the simplest scheme, superposition of these current states are generated by forward and back scattering flows of the cold atoms through a single tunnel barrier (weak link) that is achieved along the ring-shaped potential.

Following the protocols provided so far, Atomtronics flux qubits can be realized with ring-shaped BEC of typical radii of a few tens of microns. Although specific schemes for single or few coupled Atomtronics qubits can be conceived [17, 20], the actual implementations define non-trivial experimental problems in which the BEC needs to be interfaced with a laser configuration that is typically very complex. As a consequence, scalable architectures of Atomtronics qubits seem very challenging to be realized along a ‘bottom-up’ approach. Rather than pursuing such a trajectory, in this paper we apply a ‘top-down’ approach. We provide the protocol to realize a pattern of closed currents, few micron radii each, arranged in a planar configuration. Using a suitable laser configuration, we engineer a 2D optical lattice consisting of a triangular periodic array of Mexican hat potentials, trapping atoms in its ring-shaped confining wells. The scheme is completed by applying a suitable laser configuration subjecting the lattice to an effective gauge field.

We demonstrate that an effective two-level system arises, locally, in each elementary cell of the 2D lattice, that can be controlled by the effective gauge field. Overall, our system provides a scalable 2D architecture able to host Atomtronics flux qubits. We discuss specific protocols to address, couple and manipulate the two-level systems arranged in such a 2D Mexican hat lattice.

2D Mexican hat lattice laser configuration. We consider atoms (mass m , resonance frequency ω_{at} , linewidth Γ) subjected to three coplanar standing-waves lying in the xy -plane at relative angles $\pi/3$ of each other. They are produced by three retro-reflected monochromatic laser beams (same frequency ω_L) linearly-polarized along axis Oz . The corresponding wave vectors are $\vec{k}_1 = k_L(\frac{\sqrt{3}}{2}\hat{x} + \frac{1}{2}\hat{y})$, $\vec{k}_2 = k_L(-\frac{\sqrt{3}}{2}\hat{x} + \frac{1}{2}\hat{y})$, and $\vec{k}_3 = \vec{k}_1 + \vec{k}_2 = k_L\hat{y}$, with $k_L = \omega_L/c = 2\pi/\lambda_L$ (λ_L is the laser wavelength), and we assume their respective Rabi frequencies to be $\Omega_1 = \Omega_2 = \gamma\Omega$ and $\Omega_3 = \Omega$. The externally adjustable parameter γ is the relative strength of the two lateral standing-waves compared to the one along Oy . For far-detuned laser beams (detuning $|\delta_L| = |\omega_L - \omega_{at}| \gg \Gamma$), and after a suitable choice of the origin of coordinates, the light-shift potential experienced by the atoms is $V(\vec{r}) = U_0 v(\vec{r})$ where:

$$v(\vec{r}) = \left[\cos k_L y + 2\gamma \cos\left(\frac{k_L y + \phi}{2}\right) \cos\left(\frac{\sqrt{3}k_L x}{2}\right) \right]^2 \quad (1)$$

and $U_0 = \hbar\Omega^2/(4\delta_L)$. The externally adjustable parameter ϕ accounts for the phase mismatch between the standing-waves. The underlying Bravais structure of this periodic potential is triangular with a unit Bravais cell spanned by $\vec{a}_1 = \lambda_L(\frac{1}{\sqrt{3}}\hat{x} + \hat{y})$ and $\vec{a}_2 = \lambda_L(-\frac{1}{\sqrt{3}}\hat{x} + \hat{y})$, see [21] for more details. We assume here $\delta_L > 0$ (blue-detuned standing-waves), so that the potential strength U_0 is positive. In this case, the global minima of the potential solve $v(\vec{r}) = 0$. For balanced ($\gamma = 1$) and in-phase laser fields ($\phi = 0$), these minima form ring-shaped contours encircling the global maxima of the potential. In turn, the full optical potential shows up as a triangular lattice of Mexican hat structures. This Mexican hat structure is slightly distorted but maintained provided the lattice laser beams are not too much imbalanced (γ sufficiently close to unity) and almost in-phase (ϕ small enough). Fig. 1 gives a plot of $v(\vec{r})$ and of the ring structure of its minima for $\gamma = 0.98$ and $\phi = \pi/25$.

Independent lattice cells regime. When the lower bands of the Mexican hat lattice band structure are flat compared to their separation, tunneling does not couple efficiently adjacent cells. This means that atoms trapped in a given cell would stay there for a very long time and would be virtually isolated from the rest of the lattice. Providing this residence time (given by the tunneling time) is larger than the time required to manipulate and interrogate the atoms, then their local dynamics can be simply understood in the so-called atomic limit,

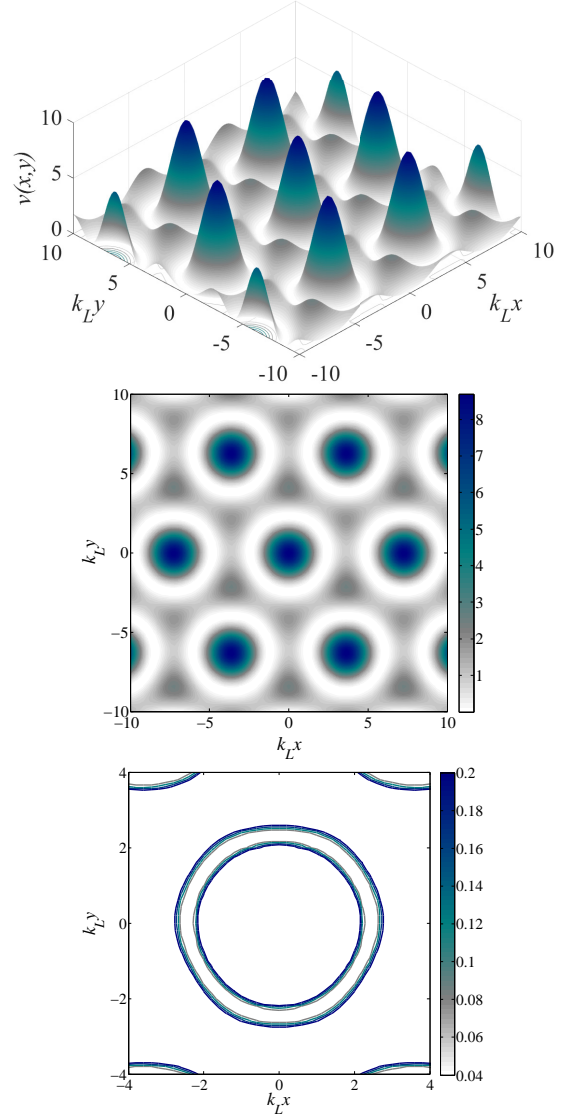


FIG. 1. (Color online) The Mexican hat triangular optical lattice obtained from the structure function $v(\vec{r})$, Eq. (1), with $\gamma = 0.98$ and $\phi = \pi/25$ (Top Panel). Sufficiently cold atoms would accumulate in the ring-shaped minima obtained for $v(\vec{r}) = 0$ (white rings in middle panel). By increasing the potential strength U_0 , tunneling between adjacent cells can be strongly suppressed and the different cells become independent. Each of them is able to store a single "flux" qubit. Bottom panel: contour plot of the (slightly distorted) ring-shaped potential well within a unit cell of the Mexican hat lattice.

that is from the local eigenstates and spectrum of the Mexican hat potential within one cell. The tunneling amplitude between adjacent cells is expected to scale like $\hbar_e^{-3/2} \exp(-S/\hbar_e)$, where S is a number (effective action) and $\hbar_e = \sqrt{2E_R/U_0}$ is the effective Planck's constant ($E_R = \hbar^2 k_L^2/(2m)$ is the recoil energy) [22]. Therefore inter-cell tunneling is exponentially suppressed with a rate proportional to $\sqrt{U_0/(2E_R)}$. At the same time, the

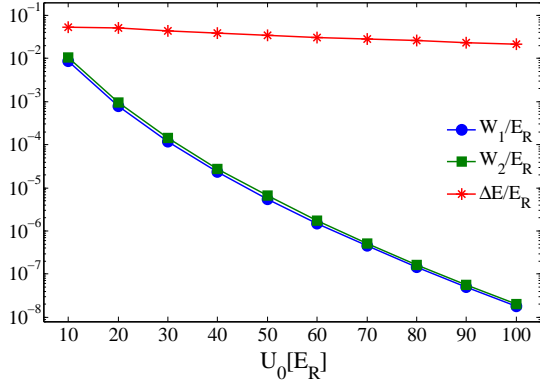


FIG. 2. (Color online) Logarithmic plot of the gap ΔE (in units of the recoil energy E_R) between the two lowest bands of the Mexican hat lattice and their respective widths W_1 and W_2 (in units of E_R) for different values of U_0/E_R . All plots are obtained with $\gamma = 0.98$ and $\phi = \pi/25$. For $U_0 \geq 50E_R$, the band widths are smaller than the band gap by at least four orders of magnitude.

band gaps is expected to scale algebraically with \hbar_e (the power law depends on the anharmonicity of the potential around its minimum). Thus, the larger U_0 the flatter the bands and the better the ratio between the band gap and the band width. Fig.2 shows our data extracted from a numerical computation of the band structure. As one can see, for $U_0 \geq 50E_R$, the band widths are smaller than the band gaps by more than four orders of magnitude.

Local qubit system. Since the lattice constant can be made large enough by an appropriate choice of the laser wavelength λ_L , individual addressing of lattice sites is feasible. Furthermore the spatial stability of the lattice, obtained by controlling the phase of the laser fields [23], would ensure the repeatability of the addressing. The basic idea, then, is to encode the atoms confined within a unit cell of the Mexican hat potential with a qubit dynamics. This can be achieved by using Laguerre-Gauss beams and 2-photon stimulated Raman processes to transfer orbital angular momentum to the atoms [24, 25]. Many-cell addressing can be done by using optical vortex arrays [26], or by using a hologram generated by a spatial light modulator [27], while individual addressing can be achieved by using a high-resolution objective and a XY-scanning AOM configuration [28].

The single-cell and single-particle Hamiltonian for this system reads

$$\mathcal{H} = \frac{(\vec{p} - \vec{A})^2}{2m} + U_0 v(\vec{r}) \quad (2)$$

where $\vec{r} = \alpha_1 \vec{a}_1 + \alpha_2 \vec{a}_2$ is restricted within a given unit Bravais cell \mathcal{B} ($|\alpha_i| \leq 1/2$, $i = 1, 2$) of the full lattice and where open boundary conditions are used ($\psi(\vec{r}) = 0$ for $\vec{r} \in \partial\mathcal{B}$). The synthetic gauge field can be chosen as $\vec{A} = -B\gamma\hat{x}$, providing an effective mag-

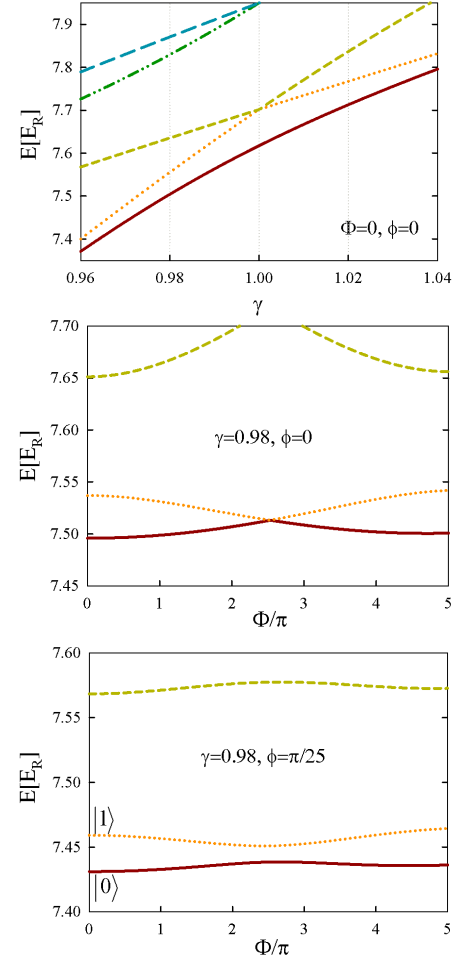


FIG. 3. (Color online) Top panel: The five lowest zero-flux energy levels of the lattice band structure at zero Bloch wave vector (in units of the recoil energy E_R) as a function of imbalance γ when $\phi = 0$. By departing γ from unity, one can separate the two lowest levels from all others. Middle panel: The three lowest single-particle energy levels (in units of the recoil energy E_R) obtained for $\gamma = 0.98$ and $\phi = 0$ within a single unit Bravais cell (with open boundary conditions) as a function of the synthetic flux Φ . The two lowest levels cross at some flux $\Phi_0 = 2.525\pi$. Bottom panel: Same as middle panel but with $\phi = \pi/25$. As one can see, the degeneracy at Φ_0 is lifted. The qubit is encoded in the two lowest states dubbed $|0\rangle$ and $|1\rangle$. For all Panels, $U_0 = 50E_R$.

netic field B along Oz and a flux per unit cell $\Phi = (\vec{\nabla} \times \vec{A}) \cdot (\vec{a}_1 \times \vec{a}_2) = 2B\lambda_L^2/\sqrt{3}$. We have duly checked that the lowest eigenenergies of this system at zero flux match with the ones obtained from the band structure of the full lattice at zero Bloch wave vector. Fig. 3 shows the dynamics of the lowest single-particle energy levels as functions of parameters γ , ϕ and flux Φ . Starting from the lattice band structure obtained at zero Bloch wave vector, we isolate two levels from all others by departing γ from unity (top panel). Choosing $\gamma = 0.98$, we next compute the dynamics of these levels against the flux Φ gen-

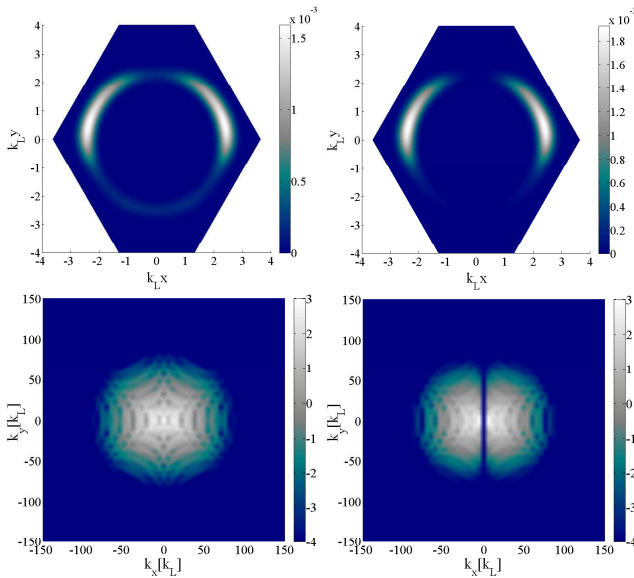


FIG. 4. (Color online) Top panels: spatial density distributions of qubit states $|0\rangle$ (left) and $|1\rangle$ (right) at zero flux $\Phi = 0$. Bottom panels: logarithm of the momentum density distributions of the same states at zero flux. Since states $|0\rangle$ and $|1\rangle$ are respectively even and odd with respect to $x \rightarrow -x$, so are their Fourier transforms with respect to $k_x \rightarrow -k_x$. Potential parameters are $U_0 = 50E_R$, $\gamma = 0.98$ and $\phi = \pi/25$.

erated by an artificial gauge field imprinted on the atoms (middle panel). The two lowest levels cross at some flux $\Phi_0 \approx 2.525\pi$. A small phase difference $\phi = \pi/25$ then serves to lift the degeneracy at Φ_0 , the third level being still sufficiently away (bottom panel). For this set of parameters, we thus get the typical level dynamics of flux qubits with an avoided crossing. We use the corresponding states, dubbed $|0\rangle$ and $|1\rangle$, to safely encode a qubit in each of the unit cells of the Mexican hat potential. By changing dynamically Φ , one is then able to perform gate operations [34–36]. Fig. 4 shows the spatial and momentum distributions of states $|0\rangle$ and $|1\rangle$. Though their spatial densities look similar, we observe that states $|0\rangle$ and $|1\rangle$ are respectively even and odd with respect to $x \rightarrow -x$. This means that their Fourier transforms are also respectively even and odd with respect to $k_x \rightarrow -k_x$. As a consequence, as seen in Fig. 4, states $|0\rangle$ and $|1\rangle$ are easily distinguishable by their momentum distributions, allowing state discrimination for quantum processing and one-qubit gates purposes.

Coupling adjacent qubits. In our architecture, this can be achieved by superposing a tailored hologram, generated by an SLM and a high-power objective, to the lattice. By modifying the tunneling barrier between the qubits, one would allow them to couple, setting the stage for two-qubit gate operations purposes [34–36]. One could even couple many different pairs of adjacent qubits in parallel. Here again, the spatial stability of the lattice potential is essential for a successful implementation of

the scheme.

Conclusion. We have proposed a simple laser scheme able to produce a scalable architecture for ring qubits placed in the elementary cells of a triangular lattice. Each qubit is rendered by a quantum particle moving in the ring-shaped minimum of a Mexican hat potential. The typical spatial extension of each qubit can be of a few microns. The 2D array of Atomtronics ring qubits can be manipulated with a logic that is formally similar to the superconducting flux qubit, but with an effective magnetic field generated by Laguerre-Gauss laser beams imprinting a synthetic gauge field on the atoms. The flux state can be determined by interference measurements [6] or by a Doppler measurement of the quantized flow state [29].

As a follow-up of our scheme, future studies should consider atom-atom interactions and address the many-body wavefunction within the ring-shaped potential minima. Assuming weak enough interactions, and correspondingly small healing length effects, the interacting (and superfluid) atoms would experience a nearly-toroidal confinement breaking the rotational symmetry because of the presence of constrictions, see bottom panel of Fig. 1. Such constrictions are known to reduce the conductance of the flowing atoms [30–32]. Since the (non-interacting) spatial distributions of the qubit states at zero flux exhibit three pinches, see Fig. 4, we conjecture that an effective description of the quantum dynamics in terms of weak links could be developed for our system, like done in [18, 33]. We would also like to point out that our scheme could be harnessed for quantum simulations of many-body systems [37]. In particular, it may provide a new perspective on vortex arrays with ultracold atoms [38, 39]. Moreover, by transferring orbital angular momentum from light to matter, it is anticipated that the scheme could be harnessed as a quantum sensor [40].

Acknowledgements This research is supported by the National Research Foundation, Prime Minister’s Office, Singapore and the Ministry of Education, Singapore under the Research Centres of Excellence programme.

-
- [1] B. Seaman, M. Krämer, D. Anderson, and M. Holland, Phys. Rev. A **75**, 023615 (2007).
 - [2] L. Amico, and M. G. Boshier, arXiv:1511.07215
 - [3] New J. Phys. **18** (2016), Focus on Atomtronics-enabled Quantum Technologies, L. Amico, G. Birkel, M. G. Boshier, and L.-C. Kwek, eds.
 - [4] S. C. Caliga, C. J. E. Straatsma, A. A. Zozulya, and D. Z. Anderson, New J. Phys. **18**, 015012 (2016).
 - [5] A. Ramanathan, K. Wright, S. Muniz, M. Zelan, W. Hill III, C. Lobb, K. Helmerson, W. Phillips, and G. Campbell, Phys. Rev. Lett. **106**, 130401 (2011).
 - [6] S. Eckel, F. Jendrzejewski, A. Kumar, C. Lobb, and G. Campbell, Phys. Rev. X **4**, 031052 (2014).
 - [7] C. Ryu, M. Andersen, P. Cladé, V. Natarajan, K.

- Helmerson, and W. Phillips, Phys. Rev. Lett. **99**, 260401 (2007).
- [8] C. Ryu and M. G. Boshier, New J. Phys. **17**, 092002 (2015).
- [9] J. Clarke and F. K. Wilhelm, Nature **453**, 1031 (2008).
- [10] I. Bloch, Nature **453**, 1016 (2008).
- [11] M. Saffman, T. Walker, and K. Mølmer, Rev. Mod. Phys. **82**, 2313 (2010).
- [12] R. Blatt, and D. Wineland, Nature **453**, 1008 (2008).
- [13] L. M. Vandersypen, M. Steffen, G. Breyta, C. S. Yannoni, M. H. Sherwood, and I. L. Chuang, Nature **414**, 883 (2001).
- [14] J. Petta, A. C. Johnson, J. Taylor, E. Laird, A. Yacoby, M. D. Lukin, C. Marcus, M. Hanson, and A. Gossard, Science **309**, 2180 (2005).
- [15] R. Dumke, M. Volk, T. Mütther, F. Buchkremer, G. Birkel, and W. Ertmer, Phys. Rev. Lett. **89**, 097903 (2002).
- [16] D. Solenov and D. Mozyrsky, J. Comput. Theor. Nanosci. **8**, 481 (2011).
- [17] L. Amico, D. Aghamalyan, F. Auksztol, H. Crepaz, R. Dumke, and L.-C. Kwek, Scientific reports **4** (2014).
- [18] D. Aghamalyan, N. Nguyen, F. Auksztol, K. Gan, M. M. Valado, P. Condylis, L.-C. Kwek, R. Dumke, and L. Amico, arXiv:1512.08376.
- [19] J. Dalibard, F. Gerbier, G. Juzeliūnas, and P. Öhberg, Rev. Mod. Phys. **83**, 1523 (2011).
- [20] D. Aghamalyan, L. Amico, and L.-C. Kwek, Phys. Rev. A **88**, 063627 (2013).
- [21] S. Safaei, C. Miniatura, and B. Grémaud, Phys. Rev. A **92**, 043810 (2015).
- [22] K. L. Lee, B. Grémaud, R. Han, B.-G. Englert, and C. Miniatura, Phys. Rev. A **80**, 043411 (2009).
- [23] C. T. Schmiegelow, H. Kaufmann, T. Ruster, J. Schulz, V. Kaushal, M. Hettrich, F. Schmidt-Kaler, and U. G. Poschinger, Phys. Rev. Lett. **116**, 033002 (2016).
- [24] M. F. Andersen, C. Ryu, P. Cladé, V. Natarajan, A. Vaziri, K. Helmerson, and W. D. Phillips, Phys. Rev. Lett. **97**, 170406 (2006).
- [25] G. Nandi, R. Walser, and W. P. Schleich, Phys. Rev. A **69**, 063606 (2004).
- [26] Y. C. Lin, T. H. Lu, K. F. Huang, and Y. F. Chen, Opt. Express **19**, 10293 (2011).
- [27] G. Gauthier, I. Lenton, N. McKay Parry, M. Baker, M. J. Davis, H. Rubinsztain-Dunlop, and T. W. Neely, arXiv:1605.04928.
- [28] H. Labuhn, S. Ravets, D. Barredo, L. Béguin, F. Nogrette, T. Lahaye, and A. Browaeys, Phys. Rev. A **90**, 023415 (2014).
- [29] A. Kumar, N. Anderson, W. D. Phillips, S. Eckel, G. K. Campbell, and S. Stringari, New J. Phys. **18**, 025001 (2016).
- [30] F. Sols and M. Macucci, Phys. Rev. B **41**, 11887 (1990).
- [31] M. W. J. Bromley and B. D. Esry, Phys. Rev. A **68**, 043609 (2003).
- [32] D. W. Sprung, H. Wu, and J. Martorell, J. App. Phys. **71**, 515 (1992).
- [33] J. Mooij, T. Orlando, L. Levitov, L. Tian, C. H. Van der Wal, and S. Lloyd, Science **285**, 1036 (1999).
- [34] Y. Makhlin, G. Schön, and A. Shnirman, Rev. Mod. Phys. **73**, 357 (2001).
- [35] H. Fan, V. Roychowdhury, and T. Szkopek, Phys. Rev. A **72**, 052323 (2005).
- [36] D. Loss and D. P. DiVincenzo, Phys. Rev. A **57**, 120 (1998).
- [37] *Quantum Simulation*, Nature Physics Insight, Nature Phys. **4** (2012).
- [38] P. Vignolo, R. Fazio, and M. P. Toni, Phys. Rev. A **76**, 023616 (2007).
- [39] A. A. Burke and E. Demler, Phys. Rev. Lett. **96**, 180406 (2006).
- [40] Thiel *et al.*, Nature Nanotechnology (2016), doi:10.1038/nnano.2016.63.